Available online at www.sciencedirect.com

SciVerse ScienceDirect

Mathematics and Computers in Simulation 108 (2015) 16–40

MATHEMATICS AND COMPUTERS IN SIMULATION

www.elsevier.com/locate/matcom

Original article

A simple financial market model with chartists and fundamentalists: Market entry levels and discontinuities

Fabio Tramontana [a,*], Frank Westerhoff [b], Laura Gardini [c]

[a] *Department of Economics and Management, University of Pavia, Italy*
[b] *Department of Economics, University of Bamberg, Germany*
[c] *Department of Economics, Society and Politics, University of Urbino, Italy*

Received 8 March 2013; received in revised form 9 June 2013; accepted 22 June 2013
Available online 12 July 2013

Abstract

We present a simple financial market model with interacting chartists and fundamentalists. Since some speculators only become active when a certain misalignment level has been crossed, the model dynamics is driven by a discontinuous piecewise linear map. Recent mathematical techniques allow a comprehensive study of the model's dynamical system. One of its surprising features is that model simulations may appear to be chaotic, although only regular dynamics can emerge. While our deterministic model is able to produce stylized bubbles and crashes we also show that a stochastic version of our model is able to match the finer details of financial market dynamics.

Keywords: Financial market crisis; Bull and bear market dynamics; Discontinuous piecewise linear maps; Border-collision bifurcations; Periodadding scheme

1. Introduction

Our paper seeks to add to the burgeoning literature on agent-based financial market models which explain the dynamics of financial markets by highlighting the trading activity of their participants. Seminal contributions in this field include Day and Huang [13], Chiarella [9], De Grauwe et al. [19], Kirman [37], Lux [43], Brock and Hommes [8], LeBaron et al. [38], Farmer and Joshi [22] and He and Li [27]. According to this class of models, interactions between heterogeneous and boundedly rational speculators, relying on simple technical and fundamental trading rules, can generate complex endogenous price dynamics, including, for instance, the emergence of bubbles and crashes. More recent approaches are surveyed in Hommes [32], LeBaron [39], Lux [44], Chiarella et al. [10] and Westerhoff [70].

A few papers in this exciting area focus on the dynamics of piecewise linear maps. Such piecewise linear maps, which may be regarded as an approximation of more complicated nonlinear maps, have the advantage that they often allow for a deeper analytical study of the underlying dynamical system, and thus advance our understanding of what is driving the dynamics of financial markets. For examples, see the asset pricing models of Huang and Day [33], Day [16], Huang et al. [34] and Tramontana et al. [67].

* Corresponding author. Tel.: +39 0382986224.
E-mail addresses: fabio.tramontana@unipv.it (F. Tramontana), frank.westerhoff@uni-bamberg.de (F. Westerhoff), laura.gardini@uniurb.it (L. Gardini).

0378-4754/$36.00
http://dx.doi.org/10.1016/j.matcom.2013.06.002

Our model, representing a stylized speculative market with interacting chartists and fundamentalists, also has a piecewise linear structure.[1] The reason for this is that we assume that while some speculators are always active in the market, others only become active when a certain misalignment level has been crossed. Since we assume otherwise linear technical and fundamental trading rules, the model consists of three disconnected branches. The inner regime is due to the transactions of speculators who are always active; the two outer regimes depend on the joint trading behavior of all market participants.

From a mathematical point of view, the peculiarity of our model is that although numerically we can observe trajectories that may look chaotic, chaotic behavior cannot occur. Instead, only regular dynamics are possible, as the trajectories are either periodic or quasiperiodic. However, both cases are structurally unstable, as they are never persistent under a parameter variation. It should also be noted that discontinuous piecewise linear maps have not yet been thoroughly studied. Despite their simplicity, they can, however, lead to surprising new insights. We hope that our paper will advance our knowledge of such maps.

From an economic point of view, our simple deterministic model is able to explain, in a qualitative sense, the excess volatility and the disconnect puzzle – which are two of the most challenging and crucial puzzles in international finance (see, e.g. Shiller [62]). We find this rather interesting since the only assumption required for this is that, in an otherwise linear world, there are different market entry levels for certain types of speculators. This assumption, which appears quite natural to us, is already sufficient for creating endogenous price dynamics. For instance, the dynamics of our model may evolve as follows. Close to the fundamental value, orders of optimistic chartists may start a bubble process. But once a certain misalignment level has been crossed, additional fundamental traders enter the market. Their orders may trigger a moderate price correction or even a stronger crash. After the fundamentalists have left the market, the remaining chartists may optimistically initiate the next bubble. However, their mood may also have turned pessimistic. In this case, they reinforce the crash. It is again the market entry of additional fundamentalists which pushes prices back to fundamental values. Moreover, we demonstrate that a stochastic version of our model is able to match the statistical properties of financial markets in finer detail. In particular, our stochastic model version is able to produce bubbles and crashes, excess volatility, fat-tailed return distributions, uncorrelated price changes and volatility clustering, thereby explaining some of the most important stylized facts of financial markets.

After these introductory remarks, the plan of the paper is as follows. In Section 2 we talk about the role of piecewise linear maps in nonlinear science. In Section 3, we introduce our model and describe some preliminary properties of its underlying dynamical system. In Section 4, we start to investigate the model in more detail. Since different parameter assumptions yield different maps, the analysis stretches over Sections 4 and 5. In Section 6 we build a stochastic version of our model, showing how it can mimic some stylized facts of actual financial markets. Finally, Section 7 concludes the paper.

2. Background for the role of piecewise linear maps in nonlinear science

It is well-known that several models in various scientific areas are represented by piecewise smooth dynamical systems. The essential feature in piecewise smooth dynamical systems, either continuous or discontinuous, is the presence of a change of definition in the functions defining the map under study, when a suitable border is met or crossed. This is at the basis of the existence of border collision bifurcations, which have been introduced (although not using this term and starting with the properties of the skew tent map) by Nusse and Yorke [54,55], Maistrenko et al. [47], Maistrenko et al. [48] and Maistrenko et al. [49]. However, also in early works by Leonov [40,41] and Mira [52,53] several properties of piecewise linear discontinuous maps have already been described, which, in turn, have recently been revisited and successfully improved by Gardini et al. [25].

Mathematical insights in this area are important since these kinds of systems have recently found a wide use in several applied fields. We recall, for example, the books by Banerjee and Verghese [4], Zhusubaliyev and Mosekilde [72] and di Bernardo et al. [20]. In particular, piecewise smooth systems are applied in power electronic circuits (Halse et al. [26], Banerjee et al. [3]), impacting systems (Nusse et al. [56], Ing et al. [35], Sharan and Banerjee [61], to cite a few), piecewise smooth nonlinear oscillators (Pavlovskaia et al. [58], Pavlovskaia and Wiercigroch [59]), cryptography

[1] Note that there is abundant empirical evidence, summarized by Menkhoff and Taylor [50], which supports the view that speculators indeed rely on technical and fundamental trading rules.

(de Oliveira and Sobottka et al. [57] and Li et al. [42]) and in many other applications (Banerjee and Grebogi [2], Sushko et al. [63,64]).

But there are also many application of continuous and discontinuous piecewise smooth maps in economics and finance. A pioneer in this field has been Richard Day, as e.g. Day [11,15], Day and Shafer [12] and Day and Pianigiani [14], whose work has been continued in Metcaf [51] and Böhm and Kaas [5], among others. In this respect, it is also worth mentioning the contributions by Hommes [28,29], Hommes and Nusse [30] and Hommes et al. [31]. Further economic and financial models can be found in Puu and Sushko [60] and Tramontana et al. [65,66].

As we will see, the model considered in this work is quite special. On the one hand, it differs from most papers listed above because it has two discontinuities. On the other hand, it differs from some known bifurcation mechanisms of piecewise linear maps because of a particular, always satisfied, "stability condition", which only implies the existence of periodic and quasiperiodic dynamic behaviors. In other words, as we will see, a chaotic motion never occurs and any small parameters' variation leads to a cycle of different period (or quasi-periodic behavior). The main point is that the economic model here described surprisingly leads exactly to this class of maps.

While our focus is on one-dimensional maps, we finally mention that piecewise linear or piecewise smooth maps in higher-dimensional spaces have also been proposed in different areas of science and economics. Besides some of the aforementioned works, see, for instance, di Bernardo et al. [21], De et al. [17,18] and Banerjee et al. [1].

3. A discontinuous financial market model

Overall, our financial market model consists of rather standard building blocks, formalizing the behavior of a market maker, and four types of speculators. A special feature of our model is that we assume that so-called type 1 chartists and type 1 fundamentalists are always active in the market, whereas so-called type 2 chartists and type 2 fundamentalists only become active when prices deviate at least a certain minimum amount from fundamentals. Note that the more unbalanced a market becomes, the more attention it indeed receives, for instance due to heightened media coverage. Popular examples in this respect include the dot-com bubble and the recent financial crisis following the Lehman debacle. On the one hand, this may trigger an additional inflow of chartists which optimistically/pessimistically speculate on a continuation of the current bull/bear market. On the other hand, there may also be an additional inflow of fundamentalists which believe they can profit from a fundamental price correction. In this paper, we thus consider an attention-based market entry of additional traders. In Appendix A, however, we also provide an alternative, profit-based market entry argument. Note that both arguments imply the same dynamical system.

Since our simple model concentrates on transactions of heterogeneous speculators, it can, with some liberty, be seen as a stylized representation of a stock, commodity or foreign exchange market. The model will be presented in Section 3.1. In Section 3.2, we will then discuss some properties of our piecewise linear maps, and related maps, which are helpful for understanding and appreciate the properties of our model.

3.1. Our model's building block

The first building block of our model describes price adjustments. Following Day and Huang [13], we assume a market maker mediates transactions out of equilibrium by providing or absorbing liquidity, depending on whether the excess demand is positive or negative. In addition to clearing the market, the market maker quotes prices according to the following rule

$$P_{t+1} = P_t + a(D_t^{C,1} + D_t^{F,1} + D_t^{C,2} + D_t^{F,2}), \tag{1}$$

where P is the log price, a is a positive price adjustment parameter, and $D_t^{C,1}$, $D_t^{F,1}$, $D_t^{C,2}$ and $D_t^{F,2}$ are the orders of the four types of speculator. Accordingly, excess buying drives the price up and excess selling drives it down. For simplicity, yet without loss of generality, we set scaling parameter a equal to 1.

Chartists believe in the persistence of bull and bear markets. The orders of type 1 chartists are therefore given by

$$D_t^{C,1} = c^1(P_t - P^*), \tag{2}$$

where c^1 is a positive reaction parameter and P^* stands for the asset's (constant) log fundamental value. Hence type 1 chartists submit buying orders in bull markets and selling orders in bear markets.[2]

The trading behavior of fundamentalists is exactly contrary to the trading behavior of chartists. We formalize the orders of type 1 fundamentalists by

$$D_t^{F,1} = f^1(P^* - P_t), \tag{3}$$

where f^1 is a positive reaction parameter. Clearly, (3) generates buying orders when the market is overvalued and generates selling orders when it is undervalued.

What type 1 chartists and type 1 fundamentalists have in common is that they are almost always active. Once they perceive a mispricing, they start trading. Type 2 chartists and type 2 fundamentalists are different to them in the sense that they only become active when the misalignment exceeds a certain critical threshold level. As already mentioned, we assume in our model an attention-based market entry of type 2 traders (and Appendix A develops a profit-based market entry argument, leading exactly to the same demand function). The orders of type 2 chartists and type 2 fundamentalists are therefore represented by

$$D_t^{C,2} = \begin{cases} 0 & \text{if} |P_t - P^*| < z \\ c^2(P_t - P^*) & \text{if} |P_t - P^*| > z \end{cases} \tag{4}$$

and

$$D_t^{F,2} = \begin{cases} 0 & \text{if} |P_t - P^*| < z \\ f^2(P^* - P_t) & \text{if} |P_t - P^*| > z \end{cases} \tag{5}$$

respectively. Again, reaction parameters c^2 and f^2 are positive and the aforementioned threshold level is given by $z > 0$.

It is convenient to express the model in terms of deviations from its fundamental value. Using auxiliary variable $X_t = P_t - P^*$ and combining (1)–(5) yields

$$X_{t+1} = \begin{cases} (1 + c^1 - f^1)X_t & \text{if} |X| < z \\ (1 + c^1 - f^1 + c^2 - f^2)X_t & \text{if} |X| > z \end{cases}, \tag{6}$$

which is a one-dimensional map consisting of three linear, disconnected straight lines.

Furthermore, it is useful to introduce definitions $S^1 = c^1 - f^1$ and $S^2 = c^2 - f^2$. Note first that S^1 and S^2 can take any values. A positive (negative) value of S^1 means that type 1 chartists are more (less) aggressive than type 1 fundamentalists. Of course, the same interpretation holds for S^2 and type 2 speculators: a positive (negative) value of S^2 now means that type 2 chartists are more (less) aggressive than type 2 fundamentalists.

At first sight, it might appear peculiar that type 2 chartists and type 2 fundamentalists become active simultaneously when the distance between the price and the fundamental value becomes larger than z and, indeed, a more general model might allow for two different threshold levels (which would result in a map with five linear branches). However, in an even simpler version of our model we can have any positive value for S^2 if we assume that there are only type 2 chartists and any negative value for S^2 if we assume that there are only type 2 fundamentalists. As we shall see later on, the latter specification, implying additional fundamentalists, is particularly interesting (and economically quite reasonable). For the moment, however, we shall stick to the more general setup which includes both type 2 chartists and type 2 fundamentalists.

To simplify the notation even further, let us write $X' = X_{t+1}$ and $X = X_t$. Then (6) can be expressed as

$$\overline{F}: \quad X' = \begin{cases} (1 + S^1)X & \text{if} |X| < z \\ (1 + S^1 + S^2)X & \text{if} |X| > z \end{cases}. \tag{7}$$

This is the map we explore in detail in the rest of the paper.

[2] This building block also goes back to Day and Huang [13]. Note that Boswijk et al. [6] and Westerhoff and Franke [71] report empirical support for such kind of trading behavior.

3.2. Some preliminary properties

First, however, it is helpful to contrast some properties of map (7) with those of the following map

$$F: \quad X' = \begin{cases} (1+S^1)X + E & \text{if} |X| < z \\ (1+S^1+S^2)X & \text{if} |X| > z \end{cases}, \tag{8}$$

where the extra parameter E can be positive or negative.[3]

A first property is that parameter z is a scale variable. In fact, by using the change of variable $x = X/z$ and defining the aggregate parameter $M = E/z$, our model in (8) becomes

$$F: \quad x' = \begin{cases} (1+S^1)x + M & \text{if} |x| < 1 \\ (1+S^1+S^2)x & \text{if} |x| > 1 \end{cases}. \tag{9}$$

That is, we have the following

Property 1. *The map in (8) is topologically conjugated to the map in (9).*

Note that M can be positive, negative or zero. However, the two cases with a positive and negative sign of M are topologically conjugated to one another. We have the following

Property 2. *The map F in (9) with $M<0$ is topologically conjugated with the same map F and $M>0$.*

In fact, by using the change of variable $y = -x$, the map in (9)) leads to

$$F: \quad y' = \begin{cases} (1+S^1)y - M & \text{if} |y| < 1 \\ (1+S^1+S^2)y & \text{if} |y| > 1 \end{cases}. \tag{10}$$

Clearly, the property holds also for map F in (8) with the sign of E. Hence, model (9) can be expressed as:

$$F: \quad x' = \begin{cases} g(x) = (1+S^1+S^2)x & \text{if} \quad x < -1 \\ f(x) = (1+S^1)x + M & \text{if} \quad -1 < x < 1 \\ g(x) = (1+S^1+S^2)x & \text{if} \quad x > 1 \end{cases}, \tag{11}$$

and is represented by a one-dimensional piecewise linear discontinuous map, with two discontinuity points.

Investigating dynamics of this kind of map is quite new, and not yet fully understood. We can therefore have some generic dynamic properties for our class of maps, which are related to the piecewise linear structure (see Tramontana et al. [68]). As we shall see, the case with $M = 0$ is very special. The numerical simulations of the observed dynamics may lead to incorrect conclusions, reflecting a sequence of states very close to chaotic behavior, although no chaos can occur. In fact, this case leads to a non-chaotic map with peculiar properties, with regular dynamics, either being periodic or quasiperiodic, and will be completely investigated in this paper.

By contrast, when $M \neq 0$, the dynamic behavior generally includes attracting cycles (structurally stable, as persistent for variation of each parameter in some interval) or truly chaotic dynamics (also structurally stable or robust, i.e. persistent under parameter variation). The most important property for these piecewise linear maps is that the appearance of cycles cannot occur via a fold (or tangent) bifurcation, as is usual in smooth maps. Instead, a cycle can appear/disappear only via a *border collision bifurcation*. This term, initially used in papers by Nusse and Yorke [54,55], is now used extensively in the literature of piecewise smooth systems. A cycle undergoes a border collision bifurcation when one of its periodic points merges with a discontinuity point.

Even if map (9) can generate cycles with periodic points in two or three of its partitions, there are only two functions involved, so that the eigenvalue of a cycle depends only on the number of periodic points in which functions $f(x)$ and $g(x)$ are applied. Moreover, the flip bifurcations are not the usual ones (we recall that for smooth maps it is associated

[3] Note that map (8) with $E \neq 0$ corresponds to a financial market model which is studied in Tramontana et al. [68].

with the appearance of a stable cycle of double period). In piecewise linear maps only *degenerate flip bifurcations* can occur, so that at the bifurcation value a whole segment of cycles of double period exists, stable but not asymptotically stable. The dynamic effects, after the bifurcation, are not uniquely defined. It is possible to have several kinds of dynamics, but often this bifurcation leads to chaotic sets, that is to cyclic chaotic intervals (see Sushko and Gardini [64]). Thus the following property holds:

Property 3. *A structurally stable cycle of map F in (9) can appear/disappear only via a border collision bifurcation. The eigenvalue of a cycle having p periodic points in the middle region ($|x|<1$) and q outside ($|x|>1$) is given by $\lambda = (1+S^1)^p(1+S^1+S^2)^q$. Only degenerate-type flip bifurcations can occur.*

Moreover, another property of map (9) is also immediate, and excludes cases which are unfeasible in the applied context, as leading to divergent trajectories. We know from Property 3 that when both slopes of functions $f(x)$ and $g(x)$ are in modulus higher than 1, then all of the possible cycles are unstable, as $|\lambda|>1$. In these cases, a piecewise linear map can only have chaotic dynamics (when bounded trajectories exist) or divergent trajectories. However, due to the particular structure of our map, when $|1+S^1|>1$ and $|1+S^1+S^2|>1$, we cannot have bounded dynamics because function $g(x)$ is linear. This implies that whatever the dynamics in the range $|x|<1$, where the map is affine, in a finite number of iterations any not fixed trajectory enters the region with $|x|>1$, where it depends on the iterations of an expanding linear function ($g(x)$, the graph of which is through the origin). The length of the interval bounded by 0 and x_t can therefore only increase at each step. The unique possible existing cycle is thus an unstable fixed point. Hence we have proved the following

Property 4. *Consider map F in (9) with $|1+S^1|>1$ and $|1+S^1+S^2|>1$. Then any initial condition different to the unstable fixed point (if existing) has a divergent trajectory.*

Economically, $|1+S^1|>1$ means either that type 1 chartists are slightly more aggressive than type 1 fundamentalists ($S^1>0$) or that type 1 fundamentalists are considerably more aggressive than type 1 chartists ($S^1<-2$). Moreover, $|1+S^1+S^2|>1$ may be interpreted in the sense that the joint impact of type 1 and type 2 chartists dominates, at least slightly, over the joint impact of type 1 and type 2 fundamentalists or that the joint impact of type 1 and type 2 fundamentalists is much stronger than the joint impact of type 1 and type 2 chartists. We learn from this, furthermore, that not only chartists but also fundamentalists can contribute to market instability.

In the statement of Property 3 we considered structurally stable cycles, which can occur only for $M \neq 0$. Depending on the values of the parameters, as such positive or negative slopes of functions f and g, we can have different dynamic properties. The possible outcomes associated with $M \neq 0$ has been investigated in Tramontana et al. [68], while the dynamics existing when $M=0$ is the object of the present study. As already remarked, the case $M=0$ is special as only structurally unstable dynamics, either periodic or quasiperiodic, can exist.

4. Non-chaotic regime at $M=0$

Let us consider map F in (11), for the particular case $M=0$, say F_0 (which corresponds to map $\overline{F}$ in (7) after the change of variable $x=X/z$):

$$F_0: \quad x' = \begin{cases} f(x) = (1+S^1)x & \text{if} \quad |x|<1 \\ g(x) = (1+S^1+S^2)x & \text{if} \quad |x|>1 \end{cases} \tag{12}$$

and keeping all of the possible values for the slopes of functions $f(x)$ and $g(x)$, that is $(1+S^1)$ and $(1+S^1+S^2)$ can be positive or negative and in modulus higher or smaller than 1. We can therefore consider the regions in the parameter space (S^1, S^2), as summarized in Fig. 1. This map is a particular case of a class of dynamical systems, whose properties have been analyzed in Gardini and Tramontana [24]. In this section we recall the main properties that hold for our specific model.

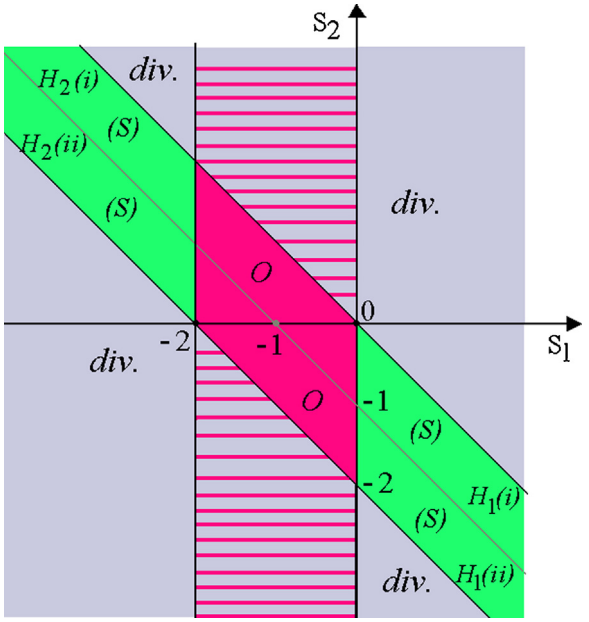

Fig. 1. Two-dimensional parameter space (S^1, S^2) at $M = 0$. The regions are bounded by straight lines $S^1 = 0$, $S^1 = -2$, $S^2 = -S^1$, $S^2 = -S^1 - 2$. Line $S^2 = -S^1 - 1$ leads only to a qualitative change. (For interpretation of the references to color in the text, the reader is referred to the web version of the article.)

Before proceeding to comment on behavior in the parameter space, let us remark on one further property specific to this case $M = 0$, which holds in the phase space of variable x. Performing the change of variable $y = -x$, the map is transformed into itself:

$$y' = \begin{cases} f(y) = (1 + S^1)y & \text{if} \quad |y| < 1 \\ g(y) = (1 + S^1 + S^2)y & \text{if} \quad |y| > 1 \end{cases} \tag{13}$$

which means that the phase space is symmetric with respect to the origin. That is: either a trajectory is symmetric with respect to the origin or the symmetric one also exists. This is particularly true for a periodic orbit. We have therefore proved the following

Property 5. *Map F_0 is invariant with respect to the change of variable $y = -x$. Thus a periodic orbit $(x_1, x_2, \ldots x_n)$ either has points symmetric with respect to the origin or $(-x_1, -x_2, \ldots -x_n)$ is also a periodic orbit.*

Let us now consider the parameter space. In Fig. 1 the regions with divergent dynamics are those already introduced in Property 4; those associated with the stability of the fixed point in origin $O = (0, 0)$ are described in the following

Property 6. *Consider map F_0 with $|1 + S^1| < 1$. For $|1 + S^1 + S^2| < 1$ fixed point O in the origin is globally attracting. For $|1 + S^1 + S^2| > 1$ fixed point O is attracting, with basin of attraction $\mathcal{B}(O) =]-1, 1[$, while any i.c. x with $|x| > 1$ has a divergent trajectory.*

In fact, if $|1 + S^1 + S^2| < 1$, then any initial condition in the range $|x| > 1$ has a trajectory which, in a few iterations, enters range $|x| < 1$ from which the trajectory converges to the origin. This leads to the red region in Fig. 1, while the dynamics in the other regions of the vertical strip of Fig. 1 are associated with $|1 + S^1 + S^2| > 1$. In such a case, any initial condition in the range $|x| < 1$ has a trajectory which converges to the origin, as it is locally stable and the map is linear in that region, while any initial condition in range $|x| > 1$, due to the structure of the piecewise linear map, has a trajectory which is divergent.

Similar to before, these cases can be interpreted economically. For instance, the unique fixed point of the model, where the price is equal to its fundamental value, is globally stable if type 1 fundamentalists are more aggressive than

type 1 chartists, but also not too aggressive ($-2 < S^1 < 0$) and also if the joint impact of both types of fundamentalists is stronger, yet not very much stronger ($S^1 + S^2$ has to remain larger than -2), than the joint impact of both types of chartist.

The particular cases with $(1+S^1)=1$ and $(1+S^1)=-1$, that is $S^1=0$ and $S^1=-2$, are *degenerate bifurcations* (as described in Sushko and Gardini [64]). For $S^1=0$ there is segment $]-1, 1[$ filled with fixed points; for $S^1=-2$ segment $]-1, 1[$ is filled with period 2 cycles. At these degenerate bifurcations, the existing cycles are stable but not asymptotically stable (i.e. they do not attract the trajectories of nearby points). After the bifurcation, for $|1+S^1|>1$, the result depends on the modulus of $(1+S^1+S^2)$. As we have seen, for $|1+S^1+S^2|>1$ only divergent dynamics can occur, while for $|1+S^1+S^2|<1$ an invariant absorbing interval J exists, given by:

$$\begin{aligned} J &= [f(-1), f(1)] = [-(1+S^1), (1+S^1)], \quad \text{if} \quad (1+S^1) > 1 \\ J &= [f(1), f(-1)] = [(1+S^1), -(1+S^1)], \quad \text{if} \quad (1+S^1) < -1, \end{aligned} \tag{14}$$

attracting the trajectories of all points of the phase space outside J (and from which a trajectory cannot escape). Thus the dynamics cannot be divergent.

It follows that the particular cases left to our analysis are exactly those in the green regions of Fig. 1, which is the main object of our work. As visible from Fig. 1, the regions under investigation are really four different regions, associated with different values of the slopes of functions $f(x)$ and $g(x)$. For $S^1>0$, these include the two cases

$$\begin{aligned} H_1(i) &: (1+S^1) > 1, \quad 0 < (1+S^1+S^2) < 1, \quad \text{increasing/increasing} \\ H_1(ii) &: (1+S^1) > 1, \quad -1 < (1+S^1+S^2) < 0, \quad \text{increasing/decreasing,} \end{aligned} \tag{15}$$

while for $S^1<-2$, these include the two cases

$$\begin{aligned} H_2(i) &: (1+S^1) < -1, \quad 0 < (1+S^1+S^2) < 1, \quad \text{decreasing/increasing} \\ H_2(ii) &: (1+S^1) < -1, \quad -1 < (1+S^1+S^2) < 0, \quad \text{decreasing/decreasing.} \end{aligned} \tag{16}$$

Again, these four regions have a simple economic interpretation. For instance, case $H_1(i)$ states that type 1 chartists are more aggressive than type 1 fundamentalists, but that the joint impact of both types of fundamentalist is stronger than the joint impact of both types of chartist. The difference between case $H_1(i)$ and case $H_1(ii)$ is that the joint impact of both types of fundamentalist is stronger in case $H_1(ii)$, yet also not too much stronger (S^1+S^2 has to remain above -2). Obviously, the main difference between the two H_1 cases and the two H_2 cases is then that the H_2 cases imply that type 1 fundamentalists are so aggressive that they destabilize the steady state within the inner regime. Global stability will, however, still be maintained as long as $|1+S^1+S^2|<1$. Given the assumption $S^1<-2$, it is then clear that aggressive type 2 chartists are required to prevent price explosions.

In the next sections, we shall fully explain cases $H_1(i)$ and $H_1(ii)$, which will also be used to explain cases H_2. Let us first introduce the peculiar property of our model described by map F_0, which is stated in the following

Property (S)**.** *Consider map* F_0 *with* $|1+S^1|>1$ *and* $|1+S^1+S^2|<1$. *Then the following equalities hold*:

$$(S): \quad f\circ g(1) = g\circ f(1) \qquad f\circ g(-1) = g\circ f(-1). \tag{17}$$

In fact, this property can be immediately verified from the definition of map F_0 given in (12): we have $g\circ f(1)=(1+S^1+S^2)(1+S^1)$ and $f\circ g(1)=(1+S^1)(1+S^1+S^2)$ as well as $g\circ f(-1)=-(1+S^1+S^2)(1+S^1)$ and $f\circ g(-1)=-(1+S^1)(1+S^1+S^2)$, so that the properties in (17) hold.

Property (S) is an important property because it leads to a *stability regime* which is, however, structurally unstable, that is: any small change in any parameter of the model leads to a different dynamic behavior. The important dynamic property of map F in this case $M=0$ is exactly this Property (S) which, as we shall see, *implies that an invariant set* I *exists, and each point of* I *has a unique rank-1 preimage in the set* I *itself.* This property (that each point of I has a unique rank-1 preimage in the set I itself) is exactly the property of a linear rotation on a circle and, depending on a suitable rotation number, which in our case is associated with the values of parameters S^1 and S^2, a trajectory may be either periodic (in which case all of the points of the interval I are periodic of the same period), or quasiperiodic and dense in the interval I. In case $H_1(i)$ (increasing/increasing), considered in the next section, there are two disjoint invariant absorbing intervals: I^R and I^L. In case $H_1(ii)$ (increasing/decreasing), considered thereafter, the invariant set I will be the union of two intervals.

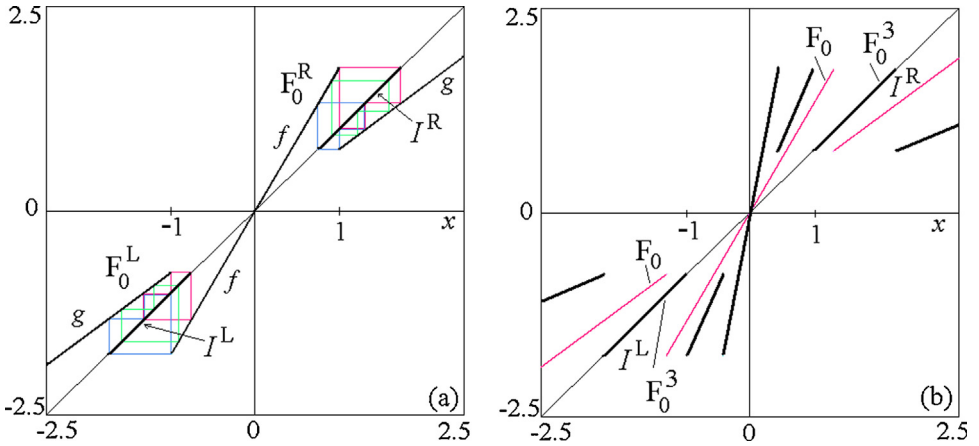

Fig. 2. Map F_0 in case $H_1(i)$ at $S^1 = 0.75$ and $S^2 = -0.9940711$ is shown in (a).

Let us analyze the conditions leading to periodic dynamics. Let x be a point belonging to the absorbing set I of map F_0, different to a discontinuity point. Then it can be a periodic point of first period n if n is the minimum integer such that $F_0^n(x) = x$. Let p be the number of periodic points of the $n-$cycle in the region $|x| < 1$ and q in the region $|x| > 1$, $(p+q) = n$. Then we have

$$F_0^n(x) = (1 + S^1)^p (1 + S^1 + S^2)^q x. \tag{18}$$

It follows that the condition of periodic orbit, $(1 + S^1)^p (1 + S^1 + S^2)^q x = x$, can be satisfied by a point $x \neq 0$ iff the eigenvalue $\lambda = (1 + S^1)^p (1 + S^1 + S^2)^q$ of the cycle satisfies the following equation

$$(1 + S^1)^p (1 + S^1 + S^2)^q = 1, \tag{19}$$

and thus the eigenvalue is $\lambda = 1$. We have so proved the following

Property 7. *Consider map F_0 with $|1 + S^1| > 1$ and $|1 + S^1 + S^2| < 1$.*

(a) *All of the trajectories enter an invariant absorbing interval I, inside which we can have either all periodic orbits or all quasiperiodic trajectories.*
(b) *The periodic orbits occur when the parameters satisfy the equation $\lambda = (1 + S^1)^p (1 + S^1 + S^2)^q = 1$ for suitable integers p and q. The proofs are given in Gardini and Tramontana [24].*

The fact that the eigenvalue of any cycle is equal to 1 means that the cycle is stable but not attracting, and in the piecewise linear case this can only occur for all points of an interval. That is, map F_0 necessarily satisfies condition $F_0^n(x) = x$ for all points x of a suitable interval, invariant for F_0^n, all points of which are periodic of the same period and with the same symbol sequence (i.e. with the same sequence of applied functions $f(x)$ and $g(x)$). Examples shall be given in the following sections, where the different cases are considered.

5. Dynamics in case $H_1(i)$, increasing/increasing

Let us consider here the effects of Property (S) for the dynamics when the map has the two functions $f(x)$ and $g(x)$, both with positive slopes $(1 + S^1) > 1$ and $0 < (1 + S^1 + S^2) < 1$, as qualitatively shown in Fig. 2a.

Under such assumptions, the map leads to two coexisting absorbing intervals, and thus *we necessarily have bistability*. In fact, any initial condition in region $x > 0$ will forever be in that region, entering the absorbing interval $I^R = [g(1),$

$f(1)]$ in a finite number of iterations, from which it cannot escape. Thus it attracts the points in $\mathcal{B}(I^R) =]0, +\infty[$, which is its basin of attraction. The restriction of map F_0 to absorbing interval I^R is given by

$$F^R: \quad x' = \begin{cases} f(x) = (1 + S^1)x & \text{if} \quad g(1) < x < 1 \\ g(x) = (1 + S^1 + S^2)x & \text{if} \quad 1 < x < f(1) \end{cases}, \tag{20}$$

where $g(1) = (1 + S^1 + S^2) \in (0, 1)$ and $f(1) = (1 + S^1) > 1$.

Similarly, any initial condition in region $x < 0$ will forever be in that region, entering the absorbing interval $I^L = [f(-1), g(-1)]$ in a finite number of iterations, from which it cannot escape, and it attracts the points in $\mathcal{B}(I^L) =]-\infty, 0[$. The restriction of map F_0 to absorbing interval I^L is given by

$$F^L: \quad x' = \begin{cases} g(x) = (1 + S^1 + S^2)x & \text{if} \quad f(-1) < x < -1 \\ f(x) = (1 + S^1)x & \text{if} \quad -1 < x < g(-1) \end{cases}, \tag{21}$$

where $f(-1) = -(1 + S^1) < -1$ and $g(-1) = -(1 + S^1 + S^2) \in (-1, 0)$.

Which kind of dynamics, then, can we have inside the two invariant absorbing intervals? Since no divergent trajectory can occur, we can argue that an initial condition in the intervals leads to some attracting set. However, this is not the case. An attracting set (or attractor) is defined as some invariant set for which a neighborhood exists whose points converge to the attractor. But this cannot occur in our map, due to the existence of property (S). In fact, it is known (as shown in [25,36]) that in the case of a piecewise smooth increasing discontinuous map, the property in (17) leads to a map which is conjugated with a linear rotation. This means that, depending on the values of S^1 and S^2, a suitable rotation number may be defined, which may be rational or irrational. For a rational rotation number, all points of absorbing intervals $I^{R/L}$ are periodic (and all of the same period). For an irrational rotation number, all points of absorbing intervals $I^{R/L}$ have quasiperiodic trajectories dense in absorbing intervals $I^{R/L}$, but are not chaotic. Thus no true attracting set can exist, but the dynamics are regular: when there are periodic orbits, these are stable but not attracting. This is also the case when there are quasiperiodic trajectories. Moreover, these dynamics are structurally unstable, as they depend on a rational or irrational rotation number, which cannot persist when varying the parameters.

An example of periodic orbits is shown in Fig. 2 for case $H_1(i)$ at $S^1 = 0.75$ and $S^2 = -0.9940711$ (the reason why this value arises is explained below). At these parameter values, all points of invariant intervals I^R and I^L are periodic of period 3 (see Fig. 2a). The third iterate of the map is shown in Fig. 2b. It consists in several branches, one of which belongs to the diagonal on invariant interval I^R, and a second branch on the diagonal on interval I^L.

The main result for our map is that *this dynamic property is always true, independent of the values of the slopes*, in the regions marked with (S) in Fig. 1. That is, for map F_0 in which we are interested, this kind of non-chaotic regime, characterized by structurally unstable orbits (either periodic or quasiperiodic), is persistent for both parameters in cases $H_1(i$ and $ii)$ and cases $H_2(i$ and $ii)$, previously defined.

Let us consider here a few more properties on the organization of the existing cycles. Property 7, in the previous section, states when a cycle can exist. However, is it possible to find the exact values of p and q that give us the cycles? And is it possible to somehow organize their existence regions (which are curves in the two-dimensional parameter plane (S^1, S^2))? The answers to both questions is positive and in Fig. 3 we can see some border collision bifurcation curves in the (S^1, S^2) parameter plane. In Appendix B we recall how to analytically obtain such curves. Under assumption $H_1(i)$, the infinitely many curves for which parameters (S^1, S^2) are associated with periodic orbits are dense in that region.

However, if we numerically compute a bifurcation diagram, we observe a figure as shown in Fig. 4, where variable x is reported as a function of S^2 at $S^1 = 0.75$ fixed. For $S^1 = 0.75$ fixed, the region corresponding to assumption $H_1(i)$ is the interval $-1.75 < S^2 < -0.75$. There we have two disjoint and coexisting invariant absorbing intervals I^R (in black in Fig. 4) and I^L (in red in Fig. 4). The numerical results are qualitatively similar to those which can be obtained in a chaotic regime. However, no chaotic regime can exist here. Since there are either periodic points or quasiperiodic trajectories at all the parameters values, and due to the fact that both the values of periodic orbits and quasiperiodic orbits are dense in the interval, we can numerically observe mainly a quasiperiodic orbit. We notice that the versus time trajectory may also be misleading. It may be considered chaotic, although this cannot be the case. An example is shown in Fig. 5. Fig. 5b shows the versus time behaviors of two coexisting trajectories, one in absorbing interval I^R and the other in absorbing interval I^L.

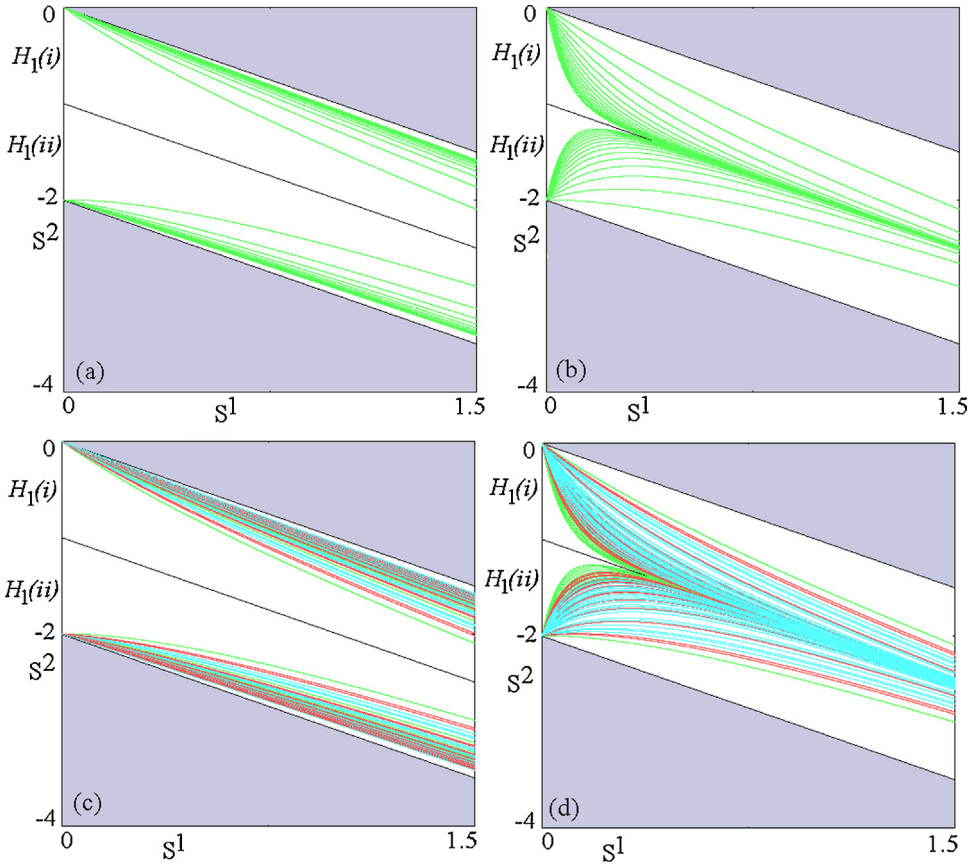

Fig. 3. Curves drawn analytically in regions $H_1(i)$ and $H_1(ii)$, as explained in the text, associated with periodic orbits of first and second complexity level. (For interpretation of the references to color in the text, the reader is referred to the web version of the article.)

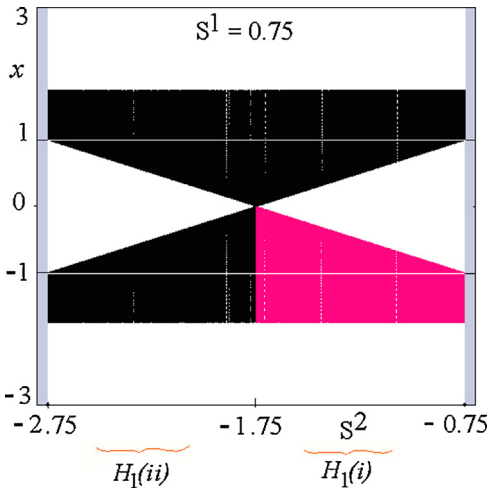

Fig. 4. One-dimensional bifurcation diagram for map F_0 showing x as a function of S^2 in both regions $H_1(i)$ and $H_1(ii)$. (For interpretation of the references to color in the text, the reader is referred to the web version of the article.)

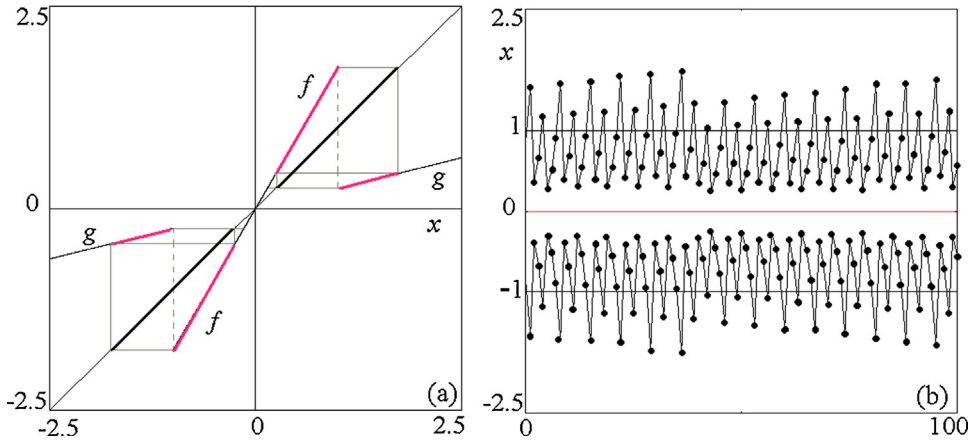

Fig. 5. Map F_0 in case $H_1(i)$ at $S^1 = 0.75$ and $S^2 = -1.5$ is shown in (a). (b) Versus time behavior of two coexisting trajectories at the same parameters as in (a).

5.1. Dynamics in the other cases

Fig. 3 also shows the bifurcation curves in region $H_1(i)$, drawn reflected in region $H_1(ii)$. That is, if parameter $(\overline{S^1}, \overline{S^2})$ belongs to a curve in region $H_1(i)$, then also the parameter which is symmetric with respect to curve $S^2 = -(1 + S^1)$ necessarily belongs to a curve in region $H_1(ii)$ associated with a periodic orbit of F_0. For example, Fig. 6 shows the 3-cycle symmetric to the 3-cycle shown in Fig. 2.

Another example is given in Fig. 7, where to the 4-cycles in region $H_1(i)$ (Fig. 7a) are associated symmetric points of 8-cycles in region $H_1(ii)$ (Fig. 7c). While the results associated with the case under assumptions $H_1(i)$ has already been proved in the literature, only recently, Gardini and Tramontana [24] proves similar results for case $H_1(ii)$ and $H_2(i, ii)$. In particular, for case $H_1(ii)$ (increasing/decreasing) Gardini and Tramontana [24] show that the dynamics are exactly the same as those described in the increasing/increasing case, and we can analytically write the curves for which we can find all periodic orbits and of any level of complexity. The property in (17) still holds, meaning that even if the map has increasing and decreasing branches (see Fig. 8), it is uniquely invertible in the invariant absorbing set, given by

$$I = [f(-1), g(1)] \cup [f(1), g(-1)]. \tag{22}$$

As a consequence of Property (S), in set I the map has either all periodic points dense in I or quasiperiodic trajectories dense in I. A numerically obtained bifurcation diagram is shown in Fig. 4 at $S^1 = 0.75$ fixed, in the region corresponding

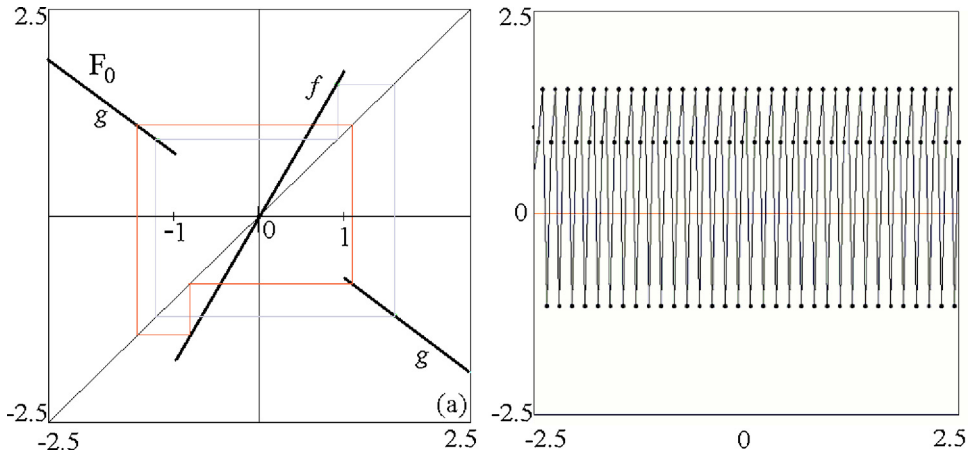

Fig. 6. Map F_0 in case $H_1(ii)$ at $(1 + S^1) = 1.75$ and $(1 + S^1 + S^2) = -0.7559289$. In (a) all points are periodic of period 3 and (b) a typical timeplot.

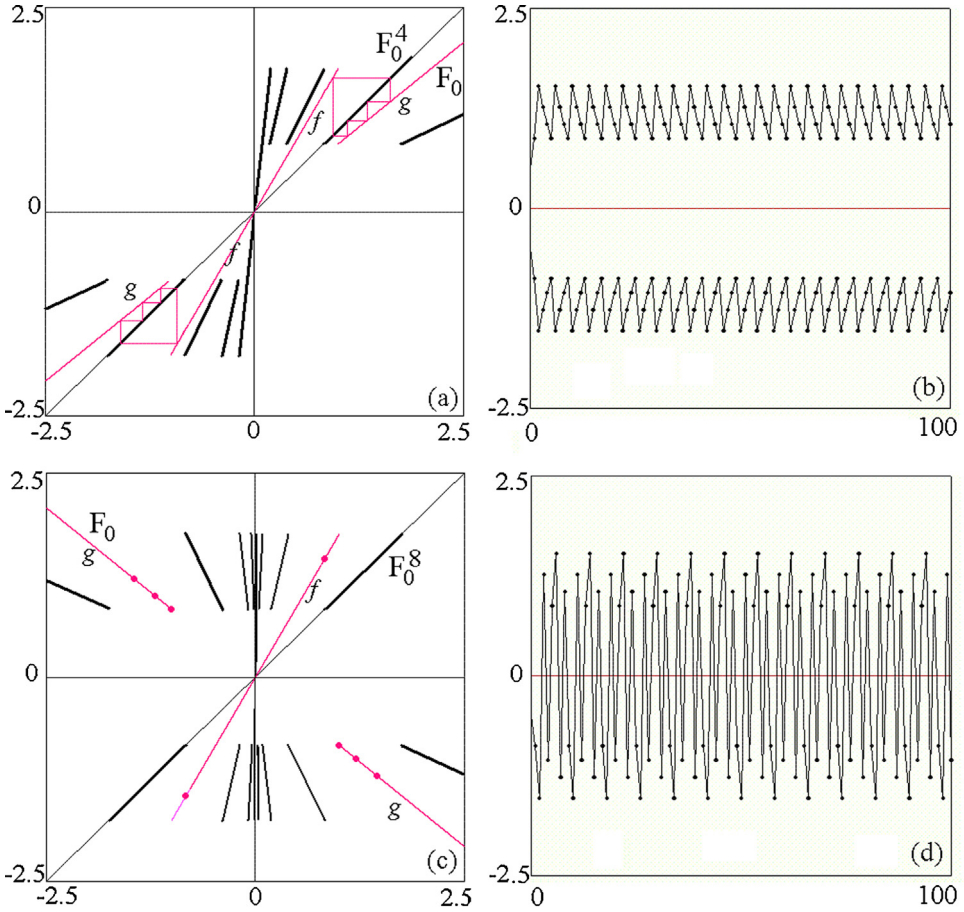

Fig. 7. Map F_0 in case $H_1(i)$ at $a = 1 + S^1 = 1.75$ and $b = 1 + S^1 + S^2 = 0.829826534$ with 4-cycles and F_0^4 are shown in (a). In (b) a timeplot. In (c) at parameters $(a, -b)$, corresponding to a point in $H_1(ii)$, there exist all 8-cycles, and F_0^8 is shown. In (d) a timeplot.

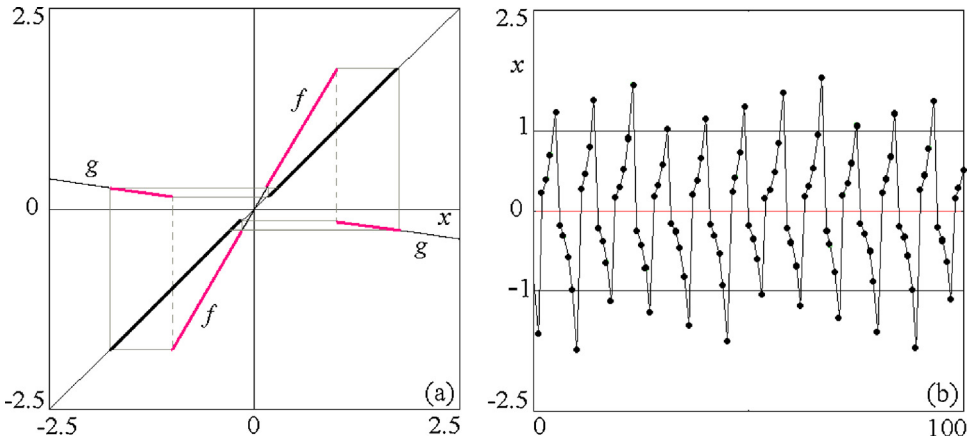

Fig. 8. Map F_0 in case $H_1(ii)$ at $S^1 = 0.75$ and $S^2 = -1.9$ is shown in (a). (b) Versus time trajectories of x at the same parameter values as in (a), in the absorbing interval I defined in (22).

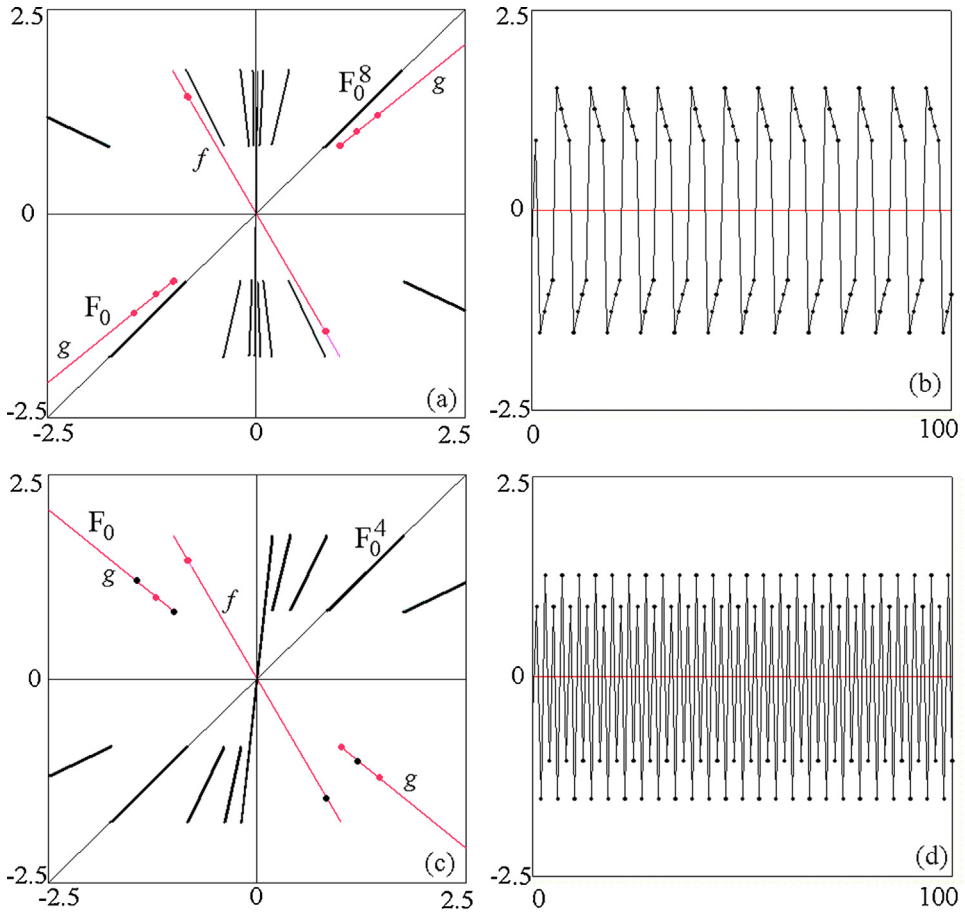

Fig. 9. Map F_0 in case $(-a, b) = (-1.75, 0.829826534)$, corresponding to a point in $H_2(i)$, shows all 8-cycles in (a), as well as F_0^8. In (b) a timeplot. In (c) the case $(-a, -b) = (-1.75, -0.829826534)$, corresponding to a point in $H_2(ii)$, we have all 4-cycles, and F_0^4 is shown. In (d) a timeplot.

to assumption $H_1(ii)$, which is the interval $-2.75 < S^2 < -1.75$. Although the figure suggests chaotic behavior, it is not. We can determine the curves associated with periodic orbits. In fact, regarding the structure of the existing cycles, we can see that in this case, in a periodic orbit function $g(x)$ is necessarily applied an even number of times. Thus on the curves of region $H_1(ii)$, which are symmetric of those of region $H_1(i)$, either the period is the same (if the number of applications of g is even (i.e. if q is even in $\overline{a}^p \overline{b}^q = \overline{(1+S^1)}^p \overline{(1+S^1+S^2)}^q = 1$) or it corresponds to a cycle of double period (see Appendix C for the technical details). Gardini and Tramontana [24] also generalize the reasoning, saying that all curves existing in region $H_1(i, ii)$ with $(1+S^1) > 1$ must also have the symmetric curves in region $(1+S^1) < -1$, in $H_2(i, ii)$, associated with periodic orbits. Ax example is given in Fig. 9 where we can see the cycles corrisponding to the 4-cycles in Fig. 7 (see Appendix C for the details).

6. A calibrated stochastic model version

So far, we have seen that our model is able to produce endogenous dynamics for a broad range of parameter values and thus has, at least in a qualitative sense, some potential to explain the emergence of bubbles and crashes and the high variability of financial markets. The goal of this section is to explore to which extend our model is able to mimic the finer details of the dynamics of actual financial markets. For a general survey about the statistical properties of actual financial markets see, for instance, Lux and Ausloos [45] and Lux and Marchesi [46].

Let us first consider Fig. 10 which visualizes the behavior of the Dow Jones Index. Since other financial markets possess quite similar statistical properties – that is the reason why these properties are called stylized facts – it is sufficient for us to restrict our attention on this particular market. The underlying time series runs from 1995 to 2012

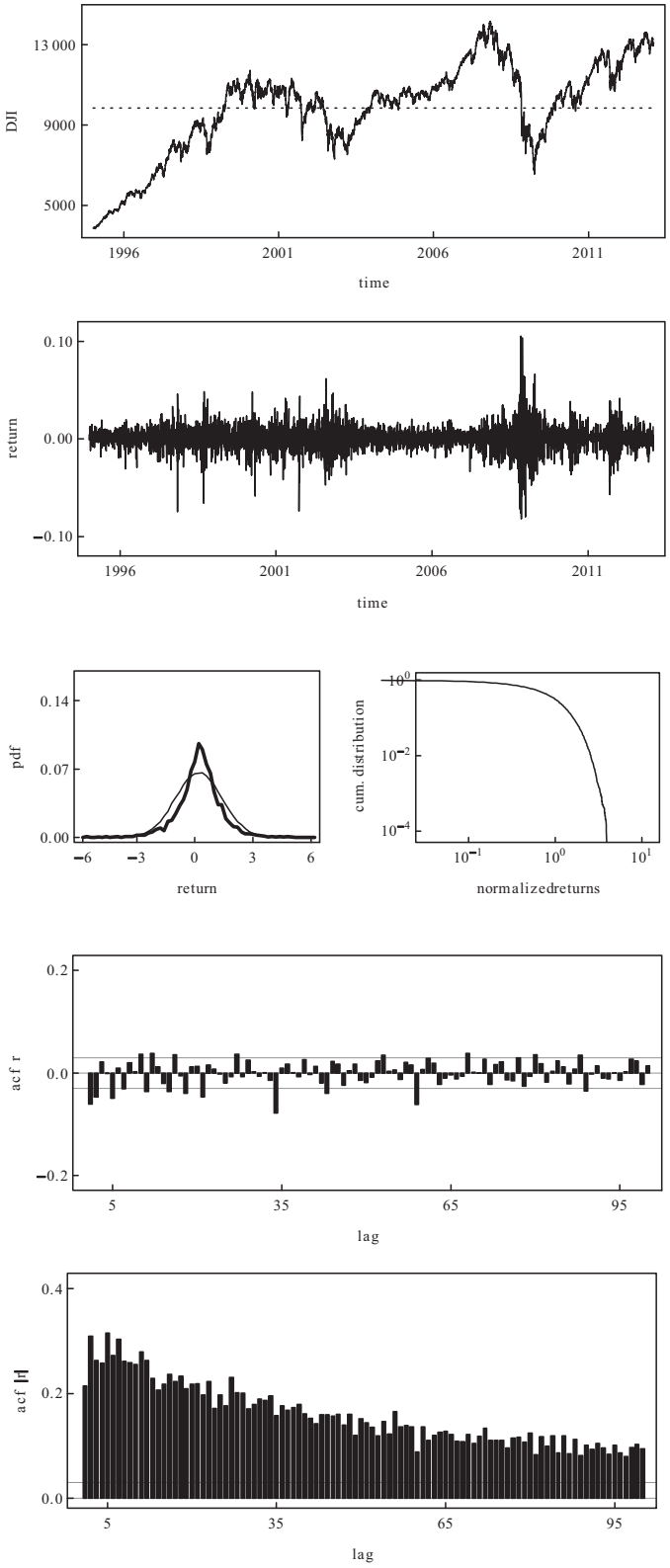

Fig. 10. The dynamics of the Dow Jones Index. The underlying time series runs from 1995 to 2012 and contains 4525 observations.

and contains 4525 observations. The top panel of Fig. 10 shows the evolution of the Dow Jones Index. Note its enormous up and down movements (the average of the Dow Jones Index is given with 9218, and displayed by the dotted line). For instance, between 1995 and 2001 the Dow Jones Index more than doubled its value while between 2007 and 2009 it lost about half its value. Such price swings are typical indicators for bubbles and crashes. The panel below presents the log changes of the Dow Jones Index, i.e. its returns. As we can see, the Dow Jones Index is quite volatile. For instance, the standard deviation of the return time series is roughly 0.12. Moreover, the returns repeatedly exceeded the 5 percent level and there are even two occasions where the Dow Jones Index increased by more than 10 percent. The left panel in the center of Fig. 10 depicts the distribution of the returns. As revealed by the thick line, the distribution of the returns of the Dow Jones Index is unimodal, almost symmetric and bell-shaped. The thin line shows normally distributed returns with identical mean and standard deviation (estimated from the returns of the Dow Jones Index). Relative to the normal distribution, we detect a higher concentration around the mean, thinner shoulders and again more probability mass in the tails of the distribution. The latter result becomes more apparent in the right panel in which the thick line presents the cumulative distribution of normalized positive and negative returns, on a log–log scale, while the thin line shows the same for standard normally distributed returns. The extra probability mass located in the tails of the return distribution of the Dow Jones Index is quite remarkable. A regression on the largest 30 percent of these observations delivers a tail index of about 3.17, providing ample evidence for the existence of a fat-tailed return distribution.

The bottom two panels contain the autocorrelation coefficients of raw returns and absolute returns for the first 100 daily lags. Note that for almost all lags the autocorrelation coefficients of the raw returns are not significant (95 percent confidence intervals are given by the thin dotted lines). Despite its boom-bust behavior, as documented by the first panel of Fig. 10, the path of the Dow Jones Index is, in a statistical sense, close to a random walk. However, the autocorrelation coefficients of absolute returns are highly significant, even after 100 lags, indicating that periods of low volatility alternate with periods of high volatility. Of course, the strong volatility clustering behavior of the Dow Jones Index is already observable in the second panel of Fig. 10.

At first sight, one could have the impression that our simple model has no chance to produce such intricate dynamics. And indeed, our deterministic model only offers a stylized explanation for bubbles and crashes and excess volatility. As we will see, however, a stochastic version of our model is capable to produce realistic dynamics. Let us turn back to our financial market model, as represented by (1)–(5), and assume that the reaction parameters of the traders as well as their perceptions of the fundamental value are subject to stochastic variations. To be more precise, let us assume that

$$\begin{aligned} c^1 &\sim N(0.150,\ 0.046),\quad f^1 \sim N(0.138, 0.046),\\ c^2 &\sim N(0.128,\ 0.043),\quad f^2 \sim N(0.150, 0.043),\\ P^* &\sim N(0,\ 0.065),\quad z = 0.2 \end{aligned}$$

Before we continue, a few remarks are in order. First, the above parameter values have been identified via a trial-and-error calibration exercise, i.e. we have systematically varied these parameters till the model dynamics appeared satisfactory to us. For more advanced techniques to estimate simple agent-based financial market models see Franke and Westerhoff [23]. Second, it seems reasonable to us that the reaction parameters of the traders and their perception of the fundamental value are not constant but may change from period to period. Neither do all traders always follow exactly their trading rules nor is the computation of the fundamental value always free of errors. Since we don't want to model the traders' deviations from their deterministic trading rules in detail, we simply assume that the reaction coefficients and the perception of the fundamental are random variables. A similar modeling strategy is adopted in Westerhoff and Franke [71] and Tramontana and Westerhoff [69].[4] Note that there are no deterministic agent-based financial market models which can jointly replicate the main stylized facts of financial markets, i.e. some kind of randomness seems to be needed in these models to obtain a good fit. Third, our specification has a clear economic interpretation, at least with respect to the means of the above random variables. According to our specification, type 1 chartists (weakly) dominate type 1 fundamentalists while type 2 fundamentalists (strongly) dominate type 2 chartists. As a result, the dynamics is within the inner regime, on average, unstable, while the dynamics is within the outer

[4] An alternative to assuming that key model parameters are random variables is to add additive noise to the main structural model equations, as is, for instance, done in Franke and Westerhoff [23].

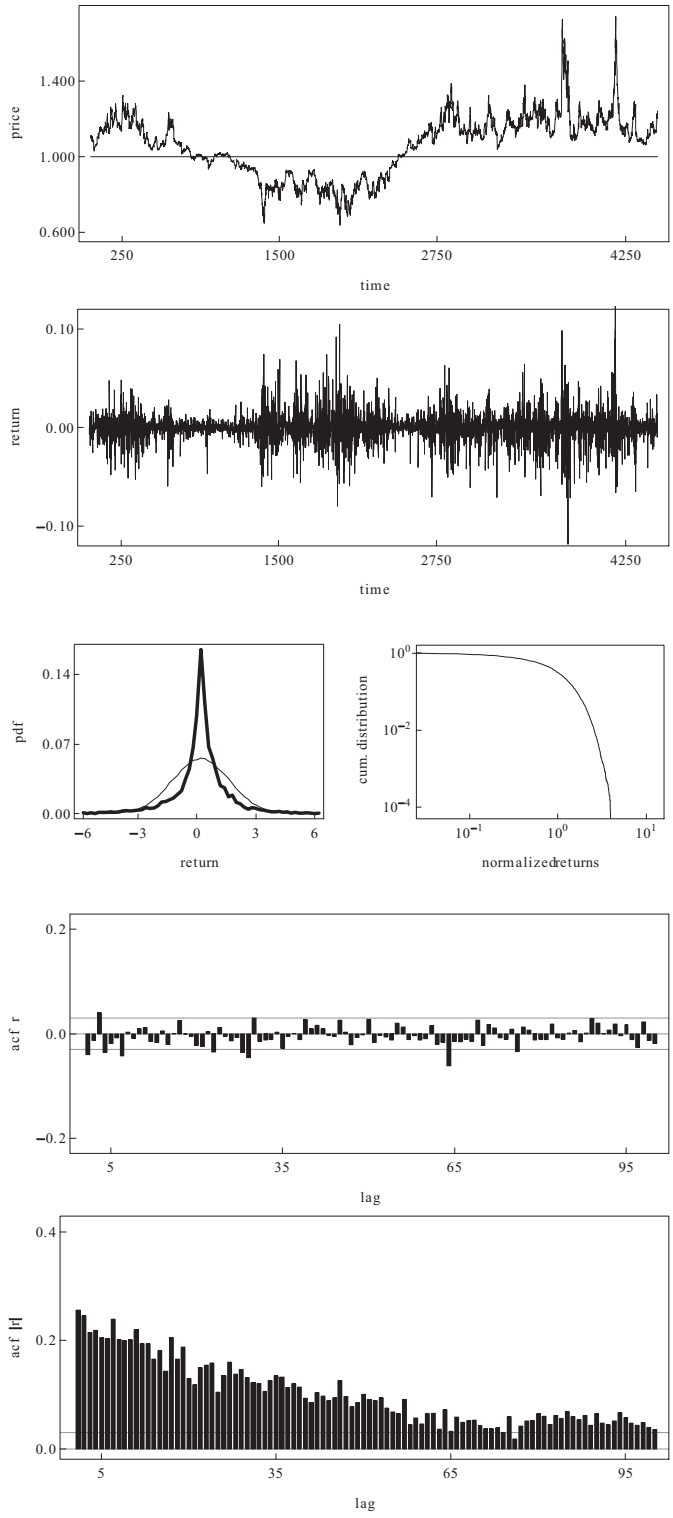

Fig. 11. A representative simulation run of our stochastic model. The underlying time series contains 4500 observations. Parameter setting as in Section 6.

regimes, on average, stable. The perceived log fundamental values vary around 0 and type 2 traders enter the market when the misalignment exceeds 20 percent.

Fig. 11 presents a typical simulation run of our stochastic model. Since the underlying time series contains 4500 observations, Fig. 11 can directly be compared with Fig. 10. The similarity between the two figures becomes immediately obvious. Our stochastic model is able to produce bubbles and crashes and excess volatility, as demonstrated by the first two panels. Prices erratically oscillate around the fundamental value with pronounced amplitude and there are a number of sharper price changes. The standard deviation of the return time series is with 0.014 slightly above what we have measured for the returns of the Dow Jones Index. Also the distribution of simulated returns is well behaved and deviates in the same way as before from normally distributed returns with identical mean and standard deviation (now estimated from simulated returns). While our simulation run possess somewhat more probability mass in the center of the return distribution, the tail behavior of simulated and actual returns is strikingly similar. For instance, the estimate of the tail index for simulated returns is given with 3.14, compared to 3.17 for the returns of the Dow Jones Index. Note also that simulated returns are hardly predictable: almost all autocorrelation coefficients of the raw returns are insignificant. In contrast, the autocorrelation coefficients of the absolute returns are clearly significant, even after 100 lags. Hence, prices essentially follow a random walk and volatility strongly clusters.

All in all, we can conclude that our stochastic model has some potential to replicate the dynamics of real financial markets. But how does the stochastic version of our model function? Recall that type 1 chartists dominate, on average, type 1 fundamentalists. Suppose that this is the case for a few consecutive time steps. As the analysis of our deterministic model reveals, the dynamics is then unstable and a monotonic price explosion sets in, at least as long as the system remains in the inner regime. But type 1 chartists only weakly dominate type 1 fundamentalists. If, by chance, type 1 fundamentalists dominate type 1 chartists, prices monotonically converge towards the fundamental value (given our choice of parameters and, of course, as long as the realizations of the random variables are not too extreme). Within the inner regime, these two scenarios alternate more or less randomly and, as a result, the price dynamics is close to a random walk process (the difference in the means of c^1 and f^1 is so small that the probability that prices increase or decrease due to a monotonic explosion or a monotonic conversion is roughly 50 percent). However, type 1 chartists are on average more aggressive than type 1 fundamentalists and therefore prices trace out a bubble path from time to time. If the dynamics enters the outer regime, the aggregate forces of type 1 and type 2 fundamentalists dominate the aggregate forces of type 1 and type 2 chartists and this brings prices eventually back to more moderate values. Since the reaction parameters of all traders are random variables, this may not appear immediately, i.e. bubbles may also build up further. Note furthermore that the price signals of chartists and fundamentalists increase with the misalignment. The farther away the price is from its fundamental value, the more aggressive is the trading behavior of the speculators. As a result, the market maker adjusts prices, due to higher excess demands, more strongly, which explains the volatility clustering phenomenon. During these periods we also observe stronger price changes, causing fat tails. Note that if prices are close to the fundamental value, misperceptions of the fundamental value may turn a bull market into a bear market or a bear market into a bull market. Therefore, prices fluctuate above and below the fundamental value (without such misperceptions, prices would stay, due to the monotonic price dynamics, either always above or always below the fundamental value).

To sum up, our simple financial market model is able to match some important statistical properties of actual financial markets. Therefore, our model may be considered as validated. Since our model rests only a minimum set of economic assumption, we find this outcome quite remarkable. We also stress that to understand the functioning of the stochastic version of our model, the analysis of the underlying deterministic model is quite helpful. Finally, our stochastic model operates at the border of stability and instability. In the future, we will explore whether also variations of parameter combinations that lead to different cycles can generate realistic dynamics. There seems to be some further potential.

7. Conclusions

In this paper we study a simple financial market model in which interactions between heterogeneous speculators can generate endogenous price dynamics. For two reasons, the model has a discontinuous piecewise linear shape: first, speculators (essentially) rely on linear technical and fundamental trading strategies. Second, while some of them are always active, others stop trading if the misalignment in the market drops below a certain threshold value. One advantage of the model's functional form is that it allows an in-depth and complete analytical investigation of its properties. We find, for instance, that the model cannot produce chaotic motions – although the dynamics appear to be

chaotic. Moreover, the model's periodic or quasiperiodic dynamics is structurally unstable, which means that any small change in any parameter of the model leads to a different dynamic behavior. Since our knowledge about discontinuous piecewise linear maps is not yet very deep, we hope that our analysis is also useful for the investigation of similar dynamical systems.

From an economic point of view, we would like to stress that it is quite remarkable that a simple model such as ours can help us to explain the emergence of bubbles and crashes. Within our model, bounded endogenous dynamics require that its steady state is unstable. As we have seen, this can be caused by either too aggressive chartists or by too aggressive fundamentalists. Further away from the steady state, the model has, of course, to be stable. Again, this can, in principle, be caused by both the market entry of additional chartists or additional fundamentalists. Additional chartists are beneficial for market stability if the steady state is destabilized by too aggressive fundamentalists while additional fundamentalists are needed for market stability if the steady state is unstable due to the trading behavior of too aggressive chartists. Despite its simplicity, it is possible to bring our model to the data. If some key model parameters are treated as random variables, the model dynamics may mimic certain properties of actual financial markets quite well. Simulations reveal, among others, virtually unpredictable prices, fat-tailed return distributions and volatility clustering.

Our model may be extended in various directions. Of course, one could assume more complex demand functions. For instance, one could allow chartists to explicitly extrapolate past price trends, which would increase the dimension of our model (the simplest case would be given by a two-dimensional system in which chartists condition their orders on the last observable price change). Alternatively, one could consider different market entry levels for chartists and fundamentalists. As a result, the model would then still be piecewise linear, but instead of having three linear branches, it would have five. Moreover, it could be interesting to explore our model's policy implications in more detail. According to conventional wisdom, it is essentially the behavior of chartists which destabilizes financial markets. A typical recommendation thus is to reduce their trading activity to obtain calmer markets. Yet, as our model shows, the trading activity of chartists can also contribute to market stability. Causalities acting inside financial markets are apparently more complicated than one is tempted to believe, indicating that more research in this direction is needed to improve our understanding of how financial markets function. And for this, a better understanding of the dynamics of discontinuous piecewise linear maps seems to be quite helpful.

Acknowledgments

This work has been performed within the activity of the project PRIN 2009 "Local interactions and global dynamics in economics and finance: models and tools", MIUR, Italy, and under the support of COST Action IS110.

Appendix A. Microfoundation of the demand functions

The goal of this appendix is to offer a brief microfoundation for demand functions (4) and (5). Instead of assuming that the market entry of type 2 traders is attention based, their market entry decision now depends on profit considerations.

Let us start with type 2 chartists. Their transactions may be expressed as

$$D_t^{C,2} = n^{C,2} w_t^{C,2} d_t^{C,2}, \tag{A.1}$$

where $n^{C,2}$ denotes the total number of type 2 chartists, $w_t^{C,2}$ the fraction of active type 2 chartists and $d_t^{C,2}$ the transaction of an active type 2 chartist.

The demand of an active type 2 chartist is formalized as

$$d_t^{C,2} = c^2(P_t - P^*). \tag{A.2}$$

Accordingly, an active type 2 trader is buying in a bull market ($P_t > P^*$) and selling in a bear market ($P_t < P^*$), with trading aggressiveness $c^2 > 0$.

The market shares of active and inactive type 2 chartists are modeled via the discrete choice approach (Brock and Hommes [7,8]). The market share of active type 2 chartists thus results as

$$w_t^{C,2} = \frac{Exp[\lambda a_t^{C,2}]}{Exp[\lambda a_t^{C,2}] + Exp[\lambda \bar{a}_t^{C,2}]}, \tag{A.3}$$

where $a_t^{C,2}$ and $\bar{a}_t^{C,2}$ indicate the attractiveness for type 2 chartists to be active or to be inactive, respectively, and parameter $\lambda > 0$ is the so-called sensitivity of choice parameter. Of course, the market share of inactive type 2 chartists is given with $(1 - w_t^{C,2})$. The main implications of (A.3) are as follows. Suppose, for instance, that $a_t^{C,2} > \bar{a}_t^{C,2}$. Then, there are more active type 2 chartists than inactive type 2 chartists. Moreover, the market share of active type 2 traders increases with λ.

For type 2 chartists, the attractiveness of being active depends on expected risk-adjusted profit opportunities and is measured as

$$a_t^{C,2} = \alpha^{C,2}|P_t - P^*| - \kappa^{C,2}, \tag{A.4}$$

where $\alpha^{C,2}$ and $\kappa^{C,2}$ are positive parameters. The first term in (A.4) captures expected profit opportunities. For a type 2 chartist, a market becomes increasingly attractive the more a bull or a bear state is developed. The second term in (A.4), i.e. parameter $\kappa^{C,2}$, accounts for the risk associated with trading.[5]

For simplicity, the attractiveness of being inactive is set to

$$\bar{a}_t^{C,2} = 0. \tag{A.5}$$

Note that the daily risk free interest rate is indeed close to zero.

In the following, we consider the so-called neoclassical limit, that is, the case in which λ goes to plus infinity (see again Brock and Hommes [7,8]). As a result, all type 2 chartists are active if $|P_t - P^*| > \kappa^{C,2}/\alpha^{C,2}$ and inactive if $|P_t - P^*| < \kappa^{C,2}/\alpha^{C,2}$. Normalizing the number of type 2 chartists to $n^{C,2} = 1$ and defining $z = \kappa^{C,2}/\alpha^{C,2}$, demand function (A.1) turns into

$$D_t^{C,2} = \begin{cases} 0 & \text{if} \quad |P_t - P^*| < z \\ c^2(P_t - P^*) & \text{if} \quad |P_t - P^*| > z \end{cases}, \tag{A.6}$$

which is formally equivalent to demand function (4).

A similar argument can easily be developed for the demand function of type 2 fundamentalists. Here, all type 2 fundamentalists switch from inactivity to activity if $|P_t - P^*|$ is about to exceed $\kappa^{F,2}/\alpha^{F,2}$. The market entry levels for type 2 chartists and type 2 fundamentalists become identical if $z = \kappa^{C,2}/\alpha^{C,2} = \kappa^{F,2}/\alpha^{F,2}$, otherwise one would obtain a discontinuous piecewise linear map with five branches.

Appendix B. Border collision bifurcation curves

In case $H_1(i)$, we can follow the same technique used in the case of attracting cycles when the so-called period adding scheme works. Indeed, as shown in Gardini et al. [25], the intersection of the existing periodicity regions with the locus (S) of the stable (but not attracting) regime where Property (S) holds is a set of points in the locus which still follows the adding mechanism. We can therefore reason similarly in our case. It is clear that, in order to have the sequence of a so-called maximal cycle in interval I^R, say with symbol sequence fg^k, we have to look for a periodic point that can be obtained as a fixed point of composite function $g^k \circ f(x)$, solving of the equation $g^k \circ f(x) = x$. For their existence we have to determine all parameters S^1 and S^2 which satisfy, for any $k \geq 1$,

$$fg^k: \qquad (1 + S^1)(1 + S^1 + S^2)^k = 1. \tag{B.1}$$

[5] Brock and Hommes [7,8] use $\kappa^{C,2}$ to model (constant) trading costs while Franke and Westerhoff [23] use $\kappa^{C,2}$ to model predisposition effects. Of course, such interpretations may also be applied in our case.

Thus we have curves in the parameter plane (S^1, S^2) given by:

$$S^2 = -(1+S^1) + \frac{1}{(1+S^1)^{1/k}}, \tag{B.2}$$

a few of which (for $k=1,\ldots,10$) are drawn in Fig. 3a. For $k=2$ we have the 3-cycles. For $S^1=0.75$, therefore, we have computed from (B.2) the value $S^2=-0.9940711$, used to draw the example in Fig. 2.

Following the adding mechanism, we can find two families of infinite curves associated with cycles of second level of complexity between any two consecutive curves associated with maximal cycles, or cycles of first level of complexity. For example, we have the following pair of families of infinite curves (both for any $m \geq 1$) between the two curves fg^k and fg^{k+1}

$$\begin{aligned} (fg^k)^m fg^{k+1} \quad &: (1+S^1)^{1+m}(1+S^1+S^2)^{k+1+mk} = 1 \\ &: S^2 = -(1+S^1) + 1/(1+S^1)^{(1+m)/(k+1+mk)} \end{aligned} \tag{B.3}$$

$$\begin{aligned} fg^k(fg^{k+1})^m \quad &: (1+S^1)^{1+m}(1+S^1+S^2)^{k+m(1+k)} = 1 \\ &: S^2 = -(1+S^1) + 1/(1+S^1)^{(1+m)/(k+m+mk)}. \end{aligned} \tag{B.4}$$

A few of these curves are shown in Fig. 3b for $k=1,\ldots,10$ and $m=1,2,3$. In Fig. 3c the curves of Fig. 3a and b are shown together (inside each pair of green curves of Fig. 3a we have those in blue and red from Eqs. (B.3) and (B.4)).

Similarly, we can continue for any level of complexity: between any two consecutive curves, with symbol sequence A and B, of the same level of complexity, we can compute two families of infinitely many curves, with symbol sequence $(A)^nB$ and $A(B)^n$, for any $n \geq 1$.

Exchanging f and g, we obtain a maximal cycle existing in interval I^R, with different symbol sequence, gf^k. A periodic point can be obtained as a fixed point of function $f^k \circ g(x)$. We therefore have to determine all parameters S^1 and S^2 such that, for any $k \geq 1$:

$$gf^k : \quad (1+S^1+S^2)(1+S^1)^k = 1 \tag{B.5}$$

and two families of curves of cycles of second complexity level are given, for any $m \geq 1$, by:

$$\begin{aligned} gf^k(gf^{k+1})^m \quad &: \quad (1+S^1+S^2)^{1+m}(1+S^1)^{k+m(1+k)} = 1 \\ &: S^2 = -(1+S^1) + 1/(1+S^1)^{(k+m+mk)/(1+m)} \end{aligned} \tag{B.6}$$

$$\begin{aligned} (gf^k)^m gf^{k+1} \quad &: \quad (1+S^1+S^2)^{1+m}(1+S^1)^{k+1+mk} = 1 \\ &: S^2 = -(1+S^1) + 1/(1+S^1)^{(k+1+mk)/(1+m)} \end{aligned} \tag{B.7}$$

and so on for any level. A few of the curves in (B.5) are drawn in region (i) in Fig. 3d for $k=1,\ldots,10$. In Fig. 3e the curves from Eqs. (B.6) and (B.7) are drawn for $k=1,\ldots,10$ and $m=1,2,3$; in Fig. 3f the curves of Fig. 3d and e are shown together.

Appendix C. Symmetry between $H_1(i, ii)$ and $H_2(i, ii)$

We state that all curves existing in region $H_1(i, ii)$ with $(1+S^1)>1$ must also have the symmetric curves in region $(1+S^1)<-1$, in $H_2(i, ii)$, associated with periodic orbits.

To show this, let us define slopes $a=(1+S^1)$ and $b=(1+S^1+S^2)$. Then let us consider parameters $(\overline{a}, \overline{b})$ corresponding to a point $(\overline{S^1}, \overline{S^2})$ belonging to a curve in region $H_1(i)$. Then also parameters $(\overline{a}, -\overline{b})$ necessarily belong to a curve associated with a periodic orbit of F_0, in region $H_1(ii)$. In fact, we know that

$$\overline{a}^p \overline{b}^q = 1 \tag{C.1}$$

for some suitable integers p and q. Then *if q is even, we also have*

$$\overline{a}^p (-\overline{b})^q = 1, \tag{C.2}$$

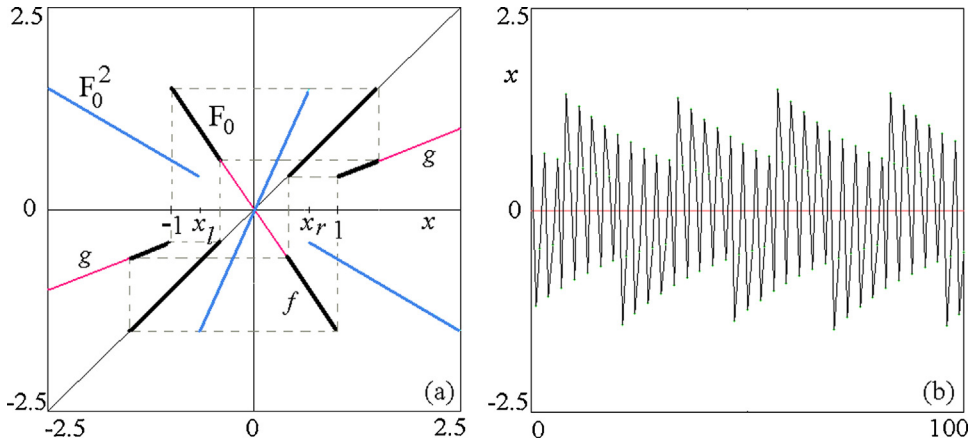

Fig. 12. Map F_0 in case $H_2(i)$ at $S^1 = -2.5$ and $S^2 = 1.9$ shown in (a). (b) Versus time trajectories of x at the same parameter values as in (a), in the absorbing interval I.

in which case the symmetric curve is associated with *a cycle of the same period* ($n = p + q$). Otherwise, *if q is odd, we have* $\overline{a}^p(-\overline{b})^q = -1$ *and*

$$\overline{a}^{2p}(-\overline{b})^{2q} = 1, \tag{C.3}$$

which means that the symmetric curve corresponds to *a cycle of double period* ($2n = 2(p + q)$).

For example, in the case of the 3-cycle shown in Fig. 2 at $(a, b) = (1.75, 0.7559289)$, we have $p = 1$ and $q = 2$, which is even. Thus we must also have 3-cycles at $(a, -b) = (1.75, -0.7559289)$, corresponding to a curve in region $H_1(ii)$, as is in fact shown in Fig. 6.

To parameters $(a, b) = (1.75, 0.829826534)$ corresponds a curve in the region $H_1(i)$ (from (B.1) with $k = 3$). The region is associated with 4-cycles with $p = 1$ and $q = 3$ which is odd (see Fig. 7a), and it follows that at $(a, -b) = (1.75, -0.829826534)$ corresponds a curve in the region $H_1(ii)$ and we must have 8-cycles, as is in fact shown in Fig. 7b.

Similarly, *if p is even, we also have*

$$(-\overline{a})^p\overline{b}^q = 1, \tag{C.4}$$

in which case the symmetric curve in region $H_2(i)$ is associated with a cycle of the same period ($n = p + q$). Otherwise, if p is odd we have $(-\overline{a})^p\overline{b}^q = -1$ and

$$(-\overline{a})^{2p}\overline{b}^{2q} = 1, \tag{C.5}$$

which means that the symmetric curve in region $H_2(i)$ corresponds to a cycle of double period ($2n = 2(p + q)$).

While considering the symmetric point in region $H_2(ii)$, we necessarily have

$$(-\overline{a})^p(-\overline{b})^q = 1 \tag{C.6}$$

when p and q are *both even or both odd*, in which case we have *cycles of the same period*, and when p and q are *one odd and one even*, from $(-\overline{a})^p(-\overline{b})^q = -1$, then we have

$$(-\overline{a})^{2p}(-\overline{b})^{2q} = 1, \tag{C.7}$$

in which case it corresponds to *cycles of double period*.

An example is shown in Fig. 8. Considering the 4-cycle in Fig. 7a, at $(a, b) = (1.75, 0.829826534)$, belonging to a curve in region $H_1(i)$ associated with 4-cycles with $p = 1$ and $q = 3$, at $(-a, b) = (-1.75, 0.829826534)$, corresponding to a point in $H_2(i)$, we must have 8-cycles, as is in fact shown in Fig. 8a. At $(-a, -b) = (-1.75, -0.829826534)$, corresponding to a point in $H_2(ii)$, we must have 4-cycles, as shown in Fig. 8b.

It is clear from the remarks given here that the curves associated with periodic orbits existing in region $H_1(i)$ (where the curves are dense) also exist in all other regions.

The dynamics in the case of assumptions $H_2(i, ii)$ are similar, since they can be reduced to those of cases $H_1(i, ii)$ using the second iterate of the map (see Gardini and Tramontana [24]).

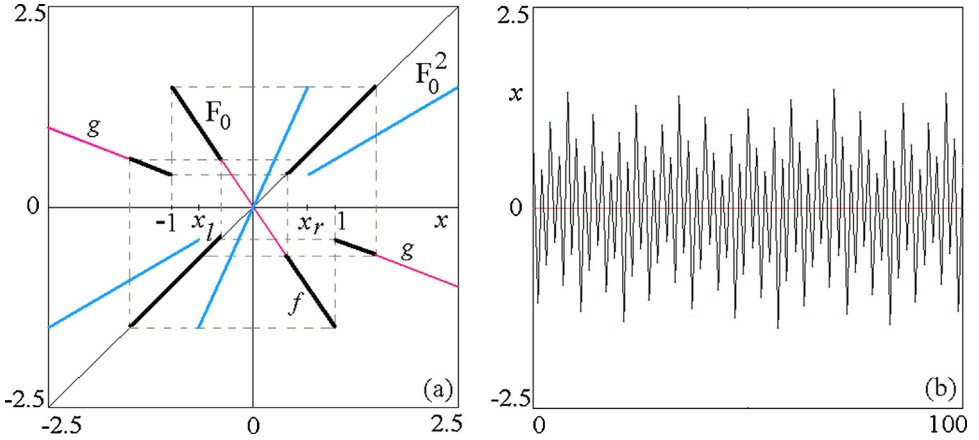

Fig. 13. Map F_0 in case $H_2(ii)$ at $S^1 = -2.5$ and $S^2 = 1.1$ is shown in (a). (b) Versus time trajectories of x at the same parameter values as in (a), in the absorbing interval I.

An example is shown in Fig. 12a. However, we notice that although the versus time dynamics of map $(F_0)^2$ when non periodic is qualitatively similar to that in Fig. 9b, the versus time dynamics of map F_0 is different, as shown in Fig. 12b. By contrast, considering case $H_2(ii)$, for the second iteration $(F_0)^2$ nothing changes in interval (x_l, x_r), where the function is $f^2(x)$. While when now we apply, outside that interval, f once and g once, the result is a positive sloped function, and the second iterate $(F_0)^2$ is a continuous function in the points $x = 1$ and $x = -1$, as we can immediately verify by direct computation, or as a consequence of Property (S). Function $(F_0)^2$ is therefore now topologically conjugated to that already considered in case $H_1(i)$, with discontinuity points in x_l and x_r in place of -1 and 1, respectively, and slopes given by $(1 + S^1)^2 > 0$ and $(1 + S^1)(1 + S^1 + S^2) > 0$ in place of $(1 + S^1)$ and $(1 + S^1 + S^2)$, respectively. That is, we have two coexisting invariant absorbing intervals, one in region $x > 0$ and the other in region $x < 0$, see Fig. 13a. However, for map F_0 there is always a unique absorbing interval I, and the states jump from the positive region to the negative one, and *vice versa*. An example of the versus time trajectory is shown in Fig. 13b.

References

[1] S. Banerjee, D. Giaouris, P. Missailidis, O. Imrayed, Local bifurcations of a quasiperiodic orbit, International Journal of Bifurcation and Chaos 22 (2012) 1250289.
[2] S. Banerjee, C. Grebogi, Border-collision bifurcations in two-dimensional piecewise smooth maps, Physical Review E 59 (1999) 4052–4061.
[3] S. Banerjee, M.S. Karthik, G.H. Yuan, J.A. Yorke, Bifurcations in one-dimensional piecewise smooth maps – theory and applications in switching circuits, IEEE Transactions on Circuits and Systems Part I 47 (2000) 389–394.
[4] S. Banerjee, G.C. Verghese (Eds.), Nonlinear Phenomena in Power Electronics: Attractors, Bifurcations, Chaos, and Nonlinear Control, IEEE Press, NY, 2001.
[5] V. Böhm, L. Kaas, Differential savings, factor shares and endogenous growth cycles, Journal of Economic Dynamics and Control 24 (2000) 965–980.
[6] P. Boswijk, C. Hommes, S. Manzan, Behavioral heterogeneity in stock prices, Journal of Economic Dynamics and Control 31 (2007) 1938–1970.
[7] W. Brock, C. Hommes, A rational route to randomness, Econometrica 65 (1997) 1059–1095.
[8] W. Brock, C. Hommes, Heterogeneous beliefs and routes to chaos in a simple asset pricing model, Journal of Economic Dynamics and Control 22 (1998) 1235–1274.
[9] C. Chiarella, The dynamics of speculative behavior, Annals of Operations Research 37 (1992) 101–123.
[10] C. Chiarella, R. Dieci, X.-Z. He, in: T. Hens, K.R. Schenk-Hoppe (Eds.), Handbook of Financial Markets: Dynamics and Evolution, Amsterdam, North-Holland, 2009, pp. 277–344.
[11] R. Day, Irregular growth cycles, American Economic Review 72 (1982) 406–414.
[12] R. Day, W. Shafer, Ergodic fluctuationsin deterministic economic models, Journal of Economic Behavior & Organization 8 (1987) 339–361.
[13] R. Day, W. Huang, Bulls, bears and market sheep, Journal of Economic Behavior & Organization 14 (1990) 299–329.
[14] R. Day, G. Pianigiani, Statistical dynamics and economics, Journal of Economic Behavior & Organization 16 (1991) 37–83.
[15] R. Day, Complex Economic Dynamics, MIT Press, Cambridge, 1994.
[16] R. Day, Complex dynamics, market mediation and stock price behaviour, North American Actuarial Journal 1 (1997) 6–21.
[17] S. De, P. Sharathi Dutta, S. Banerjee, A. Ranjan, Local and global bifurcations in three dimensional continuous piecewise smooth maps, International Journal of Bifurcation and Chaos 21 (2011) 1617–1636.

[18] S. De, P. Sharathi Dutta, S. Banerjee, Torus destruction in a nonsmooth noninvertible map, Physics Letters A 376 (2012) 400–406.
[19] P. De Grauwe, H. Dewachter, M. Embrechts, Exchange Rate Theories. Chaotic Models of the Foreign Exchange Market, Blackwell, Oxford, 1993.
[20] M. di Bernardo, C.J. Budd, A.R. Champneys, P. Kowalczyk, Piecewise-smooth Dynamical Systems, Theory and Applications, Springer-Verlag, New York, 2008.
[21] M. di Bernardo, U. Montanaro, S. Santini, Canonical forms of generic piecewise linear continuous systems, IEEE Transactions on Automatic Control 56 (2011) 1911–1915.
[22] J.D. Farmer, S. Joshi, The price dynamics of common trading strategies, Journal of Economic Behavior & Organization 49 (2002) 149–171.
[23] R. Franke, F. Westerhoff, Structural stochastic volatility in asset pricing dynamics: estimation and model contest, Journal of Economic Dynamics and Control 36 (2012) 1193–1211.
[24] L. Gardini, F. Tramontana, Structurally unstable regular dynamics in 1D piecewise smooth maps, and circle maps, Chaos, Solitons & Fractals 46 (2012) 1328–1342.
[25] L. Gardini, F. Tramontana, V. Avrutin, M. Schanz, Border collision bifurcations in 1D piecewise-linear maps and Leonov's approach, International Journal of Bifurcation and Chaos 20 (2010) 3085–3104.
[26] C. Halse, M. Homer, M. di Bernardo, C-bifurcations and period-adding in one-dimensional piecewise-smooth maps, Chaos, Solitons & Fractals 18 (2003) 953–976.
[27] X.T. He, Y. Li, Heterogeneity, convergence and autocorrelations, Quantitative Finance 8 (2008) 59–79.
[28] C.H. Hommes, Chaotic Dynamics in Economic Models, Wolters-Noodhoff, Groningen, 1991 (Ph.D. Thesis).
[29] C.H. Hommes, A reconsideration of Hick's non-linear trade cycle model, Structural Change and Economic Dynamics 6 (1995) 435–459.
[30] C.H. Hommes, H. Nusse, Period three to period two bifurcations for piecewise linear models, Journal of Economics 54 (1991) 157–169.
[31] C.H. Hommes, H. Nusse, A. Simonovits, Cycles and chaos in a socialist economy, Journal of Economic Dynamics and Control 19 (1995) 155–179.
[32] C. Hommes, in: L. Tesfatsion, K. Judd (Eds.), Handbook of Computational Economics, Agent-based Computational Economics, vol. 2, Amsterdam, North-Holland, 2006, pp. 1107–1186.
[33] W. Huang, R. Day, in: R. Day, P. Chen (Eds.), Nonlinear Dynamics and Evolutionary Economics, Oxford University Press, Oxford, 1993, pp. 169–182.
[34] W. Huang, H. Zheng, W.M. Chia, Financial crisis and interacting heterogeneous agents, Journal of Economic Dynamics and Control 34 (2010) 1105–1122.
[35] J. Ing, E. Pavlovskaia, M. Wiercigroch, S. Banerjee, Experimental study of impact oscillator with one-sided elastic constraint, Philosophical Transactions of the Royal Society A 366 (2008) 679–704.
[36] J.P. Keener, Chaotic behavior in piecewise continuous difference equations, Transactions of the American Mathematical Society 261 (1980) 589–604.
[37] A. Kirman, Ants, rationality, and recruitment, Quarterly Journal of Economics 108 (1993) 137–156.
[38] B. LeBaron, B. Arthur, R. Palmer, Time series properties of an artificial stock market, Journal of Economic Dynamics and Control 23 (1999) 1487–1516.
[39] B. LeBaron, in: L. Tesfatsion, K. Judd (Eds.), Handbook of Computational Economics, Agent-based Computational Economics, vol. 2, Amsterdam, North-Holland, 2006, pp. 1187–1233.
[40] N.N. Leonov, Map of the line onto itself, Radiofisica 3 (1959) 942–956.
[41] N.N. Leonov, Discontinuous map of the straight line, Doklady Akademii Nauk SSSR 143 (1962) 1038–1041.
[42] S. Li, G. Chen, X. Zheng, Chaos-based encryption for digital images and videos, in: B. Furht, D. Kirovski (Eds.), Multimedia Security Handbook, CRC Press, Boca Raton, Florida, 2004, pp. 110–121.
[43] T. Lux, Herd behaviour, bubbles and crashes, Economic Journal 105 (1995) 881–896.
[44] T. Lux, in: T. Hens, K.R. Schenk-Hoppe (Eds.), Handbook of Financial Markets: Dynamics and Evolution, Amsterdam, North-Holland, 2009, pp. 161–216.
[45] T. Lux, M. Ausloos, Market fluctuations I: scaling, multiscaling, and their possible origins, in: A. Bunde, J. Kropp, H.-J. Schellnhuber (Eds.), Science of Disaster: Climate Disruptions, Heart Attacks, and Market Crashes, Springer, Berlin, 2002, pp. 373–410.
[46] T. Lux, M. Marchesi, Scaling and criticality in a stochastic multi-agent model of a financial market, Nature 397 (1999) 498–500.
[47] Y.L. Maistrenko, V.L. Maistrenko, L.O. Chua, Cycles of chaotic intervals in a time-delayed Chua's circuit, International Journal of Bifurcation and Chaos 3 (1993) 1557–1572.
[48] Y.L. Maistrenko, V.L. Maistrenko, S.I. Vikul, L.O. Chua, Bifurcations of attracting cycles from time-delayed Chua's circuit, International Journal of Bifurcation and Chaos 5 (1995) 653–671.
[49] Y.L. Maistrenko, V.L. Maistrenko, S.I. Vikul, On period-adding sequences of attracting cycles in piecewise linear maps, Chaos, Solitons & Fractals 9 (1998) 67–75.
[50] L. Menkhoff, M. Taylor, The obstinate passion of foreign exchange professionals: technical analysis, Journal of Economic Literature 45 (2007) 936–972.
[51] C.J. Metcaf, The dynamics of the Stiglitz policy in the RSS model, Chaos, Solitons & Fractals 37 (2008) 652–661.
[52] C. Mira, Sur les structure des bifurcations des diffeomorphisme du cercle, Comptes Rendus de l'Académie des Sciences – Series A 287 (1978) 883–886.
[53] C. Mira, Chaotic Dynamics, World Scientific, Singapore, 1987.
[54] H.E. Nusse, J.A. Yorke, Border-collision bifurcations including period two to period three for piecewise smooth systems, Physica D 57 (1992) 39–57.

[55] H.E. Nusse, J.A. Yorke, Border-collision bifurcations for piecewise smooth one-dimensional maps, International Journal of Bifurcation and Chaos 5 (1995) 189–207.
[56] H.E. Nusse, E. Ott, J.A. Yorke, Border collision bifurcations: an explanation for observed bifurcation phenomena, Physical Review E 49 (1994) 1073–1076.
[57] L.P. de Oliveira, M. Sobottka, Cryptography with chaotic mixing, Chaos, Solitons & Fractals 35 (2008) 466–471.
[58] E. Pavlovskaia, M. Wiercigroch, C. Grebogi, Two-dimensional map for impact oscillator with drift, Physical Review E 70 (2004) 036201.
[59] E. Pavlovskaia, M. Wiercigroch, Low dimensional maps for piecewise smooth oscillators, Journal of Sound and Vibration 305 (2007) 750–771.
[60] T. Puu, I. Sushko, Oligopoly Dynamics Models and Tools, Springer-Verlag, New York, 2002.
[61] R. Sharan, S. Banerjee, Character of the map for switched dynamical systems for observations on the switching manifold, Physics Letters A 372 (2008) 4234–4240.
[62] R. Shiller, Irrational Exuberance, 2nd ed., Princeton University Press, Princeton, 2005.
[63] I. Sushko, A. Agliari, L. Gardini, Bistability and border-collision bifurcations for a family of unimodal piecewise smooth maps, Discrete & Continuous Dynamical Systems, Series B 5 (2005) 881–897.
[64] I. Sushko, L. Gardini, Degenerate bifurcations and border collisions in piecewise smooth 1D and 2D maps, International Journal of Bifurcation and Chaos 20 (2010) 2045–2070.
[65] F. Tramontana, L. Gardini, T. Puu, Duopoly games with alternative technologies, Journal of Economic Dynamics and Control 33 (2009) 250–265.
[66] F. Tramontana, L. Gardini, P. Ferri, The dynamics of the NAIRU model with two switching regimes, Journal of Economic Dynamics and Control 34 (2010) 681–695.
[67] F. Tramontana, F. Westerhoff, L. Gardini, On the complicated price dynamics of a simple one-dimensional discontinuous financial market model with heterogeneous interacting traders, Journal of Economic Behavior & Organization 74 (2010) 187–205.
[68] F. Tramontana, F. Westerhoff, L. Gardini, One-dimensional maps with two discontinuity points and three linear branches: mathematical lessons for understanding the dynamics of financial markets, Decisions in Economics and Finance (2013), http://dx.doi.org/10.1007/s10203-013-0145-y (forthcoming).
[69] F. Tramontana, F. Westerhoff, One-dimensional discontinuous piecewise-linear maps and the dynamics of financial markets, in: G.I. Bischi, C. Chiarella, I. Sushko (Eds.), Global Dynamics in Economics and Finance. Essays in Honour of Laura Gardini, Springer, Berlin, 2013, pp. 205–227.
[70] F. Westerhoff, in: J.B. Rosser Jr. (Ed.), Handbook of Research on Complexity, Edward Elgar, Cheltenham, 2009, pp. 287–325.
[71] F. Westerhoff, R. Franke, Converse trading strategies, intrinsic noise and the stylized facts of financial markets, Quantitative Finance 12 (2012) 425–436.
[72] Z.T. Zhusubaliyev, E. Mosekilde, Bifurcations and Chaos in Piecewise-smooth Dynamical Systems, World Scientific, Singapore, 2003.